Asian Journal of Chemistry; Vol. 25, No. 14 (2013), 8057-8060

ASIAN JOURNAL OF CHEMISTRY

http://dx.doi.org/10.14233/ajchem.2013.15041

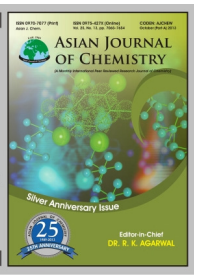

Preparation and Characterization of an Unsupported Nano-MoS_2 Catalyst

YUQIN ZHU and FAN GUO*

School of Chemistry & Chemical Engineering, Xian Shiyou University, Xian, P.R. China

*Corresponding author: Fax: +86 29 68905893; Tel: +86 13572193033; E-mail: 54394792@qq.com

(*Received*: 27 December 2012; *Accepted*: 1 August 2013) AJC-13872

Nano-sized unsupported MoS_2 hydrodesulphurization catalysts were synthesized using a novel and mainly hydrothermal, reduction method. The structures of the catalysts, their specific surface areas, mean particle sizes and micro-morphologies were characterized and analyzed. It was the first time that MoS_2 with a specific surface area of as high as 412 m^2 g^{-1} area was obtained successfully. Most of the MoS_2 had the shape of stacked platelets (slab < 8), which were between 30 and 40 nm long and 2.0 to 3.5 nm in diameter. It was found that the MoS_2 fibres were readily-flexed and contained many defects, which increased the number of active sites on the catalyst: thus they were easily able to meet the requirements of deep hydro-treatment type desulphurization of diesel oil.

Key Words: MoS_2, Unsupported catalyst, Hydro-treatment desulphurization, Diesel oil.

INTRODUCTION

With the energy savings and environmental protection requirements being strictly regulated in recent years, developed countries have accelerated the uptake of super-low sulphur gasoline and diesel fuels for their vehicles. The sulphur content of China's vehicle emissions is also gradually meeting the third type standard of the pertinent World Fuel Regulations[1]. Although various techniques of clean gasoline and diesel fuel production are emerging, the main one in the petrochemical industry remains hydro-treatment catalysis. Traditionally supported catalysts, which have been used for the desulphurization of gasoline and diesel fuels, cannot meet the requirements of the World Fuel Regulations. Therefore research effort is increasingly devoted to the development of unsupported catalysts. Thus far, the research on unsupported catalysts mainly encompasses: metal phosphides, metal carbon compounds and metal sulphides[2-9]. Generally, active components of non-sulphide hydro-treatment catalysts areoxides. According to experience and theoretical research, these hydro-treatment catalysts have higher activity when active components exist as sulphides. Therefore non-sulphide hydro-treatment catalysts must be pre-sulphurized before use. The process ensures that the active components of the catalyst react with hydrogen sulphide at a given temperature and thereby change oxides into sulphides.

There is no need to add toxic sulphur compounds to unsupported metal sulphide catalyst; the application process is relatively simple and the metal sulphide catalyst forms the basis for the principal development direction of hydrogenation catalysts.

In this paper, nano-sized unsupported MoS_2 catalysts for the deep desulphurization of diesel oil were characterized and synthesized by a hydrothermal reduction method and a high temperature hydrogen sulphide deoxidization method.

EXPERIMENTAL

The hydrothermal reduction was used to prepare MoO_3, the forming body of the MoS_2 catalyst:the nano-MoS_2 catalyst is then synthesized by hydrothermal deoxidization which is subsequently compared with high-temperature hydrogen sulphurization.

Materials for the hydrothermal reduction based preparation of MoO_3(MoO_3-Hy), of high-temperature hydrogen sulphurization to produce MoS_2(MoS_2-D) and of hydrothermal deoxidization to synthesise MoS_2 are shown in Tables 1-3, respectively. Five types of nano-MoS_2 catalysts (denoted by MoS_2-A, MoS_2-A2, MoS_2-A3, MoS_2-B and MoS_2-C) were produced by hydrothermal deoxidization.

TABLE-1
MATERIALS FOR THE PREPARATION OF MoO_3 BY HYDROTHERMAL REDUCTION

Material	Specification (%)
Hydrochloric acid	37
Sodium molybdate	≥ 99.5

TABLE-2
MATERIALS FOR THE PREPARATION OF MoS_2 BY HYDROGEN SULPHURATION

Material	Specification (%)
Hydrochloric acid	37
Sodium hydroxide	98
Hydrogen	99.99
Sodium sulphide nonahydrate	≥ 98
Nitrogen	99.99
Sodium molybdate	≥ 99.5

TABLE-3
MATERIALS FOR THE PREPARATION OF MoS_2 BY HYDROTHERMAL DEOXIDISATION

Material	Specification (%)
Hydrochloric acid	37
Nitrogen	99.99
Alcohol	95
MoO_3	≥ 99.5
Sodium sulphidenonahydrate	≥ 98

Preparation methods

Hydrothermal reduction for the preparation of MoO_3: The mixture of sodium molybdate and hydrochloric acid (state proportions here) was placed in the centre of a reactor and heated from ambient temperature to 150 ºC at an appropriate rate. The reaction temperature was maintained for 6 h and then the reactor's inner core was rapidly removed and cooled to ambient temperature to end the hydrothermal reaction. Deionized water was added to the solution to remove sodium ions by high-speed centrifugation. Finally, the precipitant was placed in an oven for several hours and a quantity of pale blue, high purityMoO_3 obtained.

High temperature hydrogen sulphuration for the synthesis of MoS_2: Sodium sulphide nonahydrate was added, from a dropping funnel, to a three-necked flask containing hydrochloric acid: hydrogen and nitrogen were then added to produce H_2S gas. Then water vapour was removed from the gaseous H_2S in a two-necked flask filled with SiO_2 desiccant. The MoO_3 was allowed to react with the gaseous H_2S at a high temperature for 2 h in a muffle furnace, while simultaneously recycling the drained-off gas through an NaOH solution. Continual addition of H_2, N_2 and H_2S to the muffle furnace was undertaken until the temperature had decreased to ambient levels. Finally the product was put in a drying oven with N_2 protection.

Hydrothermal deoxidization for synthesizing MoS_2: The mixture of MoO_3 granules, sodium sulphide nonahydrate and hydrochloric acid (state the proportions here) was put into the centre of a high-temperature reactor and heated to 250 ºC at an appropriate rate. The temperature was maintained for 6 h to ensure that the reactions' completion. The reactor core was then removed rapidly to stop the hydrothermal reaction. Deionized water and alcohol were added to the solution of the reaction products to remove sodium ions in the solution by high-speed centrifugation. The black product was then heated, washed and filtered in the reactor's oil bath. Air was pumped continually to maintain a partial vacuum and nitrogen was added to dry the black product (MoS_2) for 24 h. Finally, the MoS_2 powder arising was preserved in a dryer.

RESULTS AND DISCUSSION

Fig. 1 shows the FT-IR spectra of MoO_3(MoO_3-Hy) produced by hydrothermal reduction, of MoO_2 produced by hydrogen reduction with MoO_3 and of MoS_2-A3 by hydrothermal deoxidization, respectively. Their infrared spectra near 3450, 2356 and 1615 cm^{-1} have been absorbed to varying degrees, corresponding to the asymmetric stretching vibration of the adsorbed water, asymmetric stretching vibration of carbon dioxide and bending deformation vibration of water. The reason is that the sulphide still contained a small amount of water despite the drying process. There was significant Mo-O infrared absorption of MoO_3 at 580.1, 872.1 and 998.6 cm^{-1}; absorption peaks did not appear for MoO_2 within the measurement range of 4000-400 cm^{-1}, indicating that MoO_2 might not have infrared activity. There was still an absorption peak at 3237.4 cm^{-1} for MoO_3, which was caused by the symmetric stretching vibration of OH groups of crystalline water in the MoO_3 powder, but there was no evidence of the absorption peak in commercially available MoO_3 powder. Complex infrared absorption of MoS_2-A3 appeared at 466.7, 556.2, 671.8, 928.9 and 1166.5 cm^{-1} to varying extents. This was basically consistent with the infrared spectra of molybdenum disulphide when produced by ammonium molybdate thermal decomposition[8], indicating that MoO_3, the basis for the formation of the MoS_2, can be completely turned into MoS_2 under condition using Na_2S and HCl as reactants and solvents in the hydrothermal reduction process.

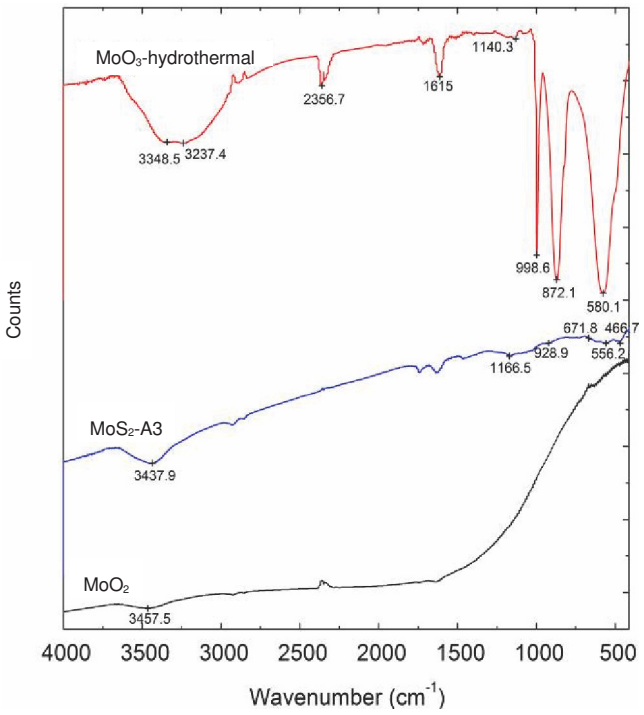

Fig. 1. Fourier infrared spectra of MoO_3, MoO_2 and MoS_2

Fig. 2 shows laser Raman spectra of MoO_3, MoS_2-A3 and MoS_2-D.Mo-O vibration characteristic peaks of MoO_3 (290, 335.7, 667.1, 819.6 and 994.8 cm^{-1}) were completely consistent with reference values in the literature[9]; the peak's shape, sharpness and signal strength, all indicated a well-crystallized oxide powder.

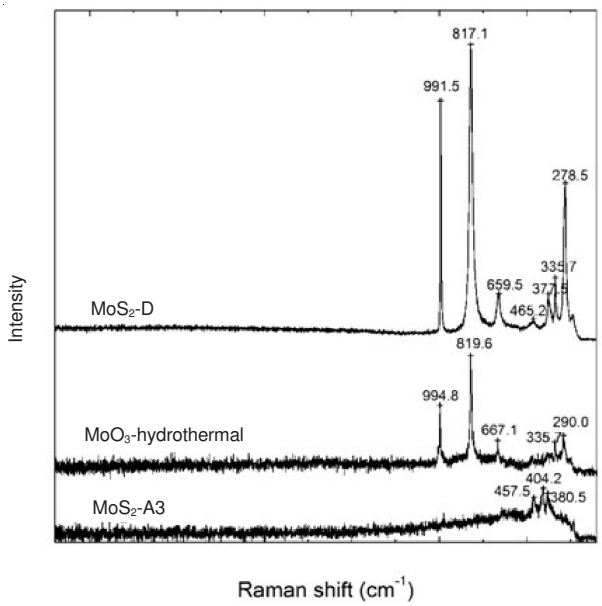

Fig. 2. Laser Raman spectra of MoO_3, MoS_2-A3 and MoS_2-D

The vibration characteristic peaks of MoS_2-D were basically consistent with Mo-O in MoO_3 except between 377.5 and 465.2 cm^{-1}, this indicated that there were also Mo-O groups in the MoS_2-D. The Mo-O characteristic peak intensity of MoS_2-D was, additionally, higher and more accurate than that of MoO_3, indicating that the crystal growth of Mo-O groups in MoS_2-D was better than in MoO_3.The MoS_2-D was produced by high-temperature hydrogen sulphuration of MoO_3, which may have led to further crystal growth by sintering of the powder during the high-temperature treatment process. There were characteristic peaks of Mo-S groups in molybdenum sulphide between 377.5 and 465.2 cm^{-1}. So there were at least two types of Mo-O and Mo-S groups in the MoS_2-D sample.

The characteristic vibration of MoS_2-A3 only appeared at 380.5, 404.2 and 457.5 cm^{-1}. This was completely consistent with the vibration of MoS_2 reported in the literature[9], indicating that the MoS_2-A3 was composed of MoS_2, just as its FT-IR analysis results showed. That is to say, MoO_3 had been completely transformed into MoS_2 through Na_2S and HCl solvent action and hydrothermal reduction treatment above 200 ºC. The characteristic peak intensity of MoS_2-A3 was very low and the peak shape was wider, which may have been caused by two reasons as follows: the powder particles produced by hydrothermal reduction synthesis being extremely fine because of particle effects and the crystallinity of MoS_2-A3 being poor.

Low temperature N_2 physical adsorption: The authors measured the specific surface area of the sulphide molybdenum powder by low-temperature nitrogen physical adsorption static capacity method (BET method); salient data are shown in Table-4. The results showed that, under low-temperature and low-concentration ratio conditions, that MoS_2-A produced byhydrothermal reduction had the highest specific surface area (412.3 m^2 g^{-1}). When the synthesis temperature increased to more than 250 ºC, the specific surface area of MoS_2-A decreased rapidly. The specific surface area of MoS_2-B was 15.9 m^2 g^{-1} at a high concentration ratio, this indicated that a high degree of crystal growth of MoS_2-B powder may have occurred or that there was significant stacking and re-joining

TABLE-4
SPECIFIC SURFACE AREAS OF MOLYBDENUM SULPHIDE

Samples	MoS_2-A	MoS_2-B	MoS_2-C
Specific surface area (m^2 g^{-1})	412.3	15.9	63.8

of powders and flocs thereof. The specific surface area for the molybdenum sulphide powder was similar to published reference values[9].

The transmission electron microscopic image of MoS_2-D is shown in Fig. 3. It shows that this MoS_2-D was composed of a large MoO_2 crystal, which was long, fibrous and clavate (*i.e.* greater than 2 μm long and of 103 nm average width).The growth orientation of these crystals was irregular, there were many small, filamentous crystals especially at the edges: these were tiny and their growth orientation lay parallel to the surface normal. These small crystals were shown to be nano-molybdenum sulphide crystals by further electron diffraction analysis. The outer surface of the MoO_2 crystals showed a thin layer presence of MoS_2.The TEM analysis also confirmed that there was more MoS_2 in the MoS_2-D sample. The results were consistent with the aforementioned Raman spectrum analysis.

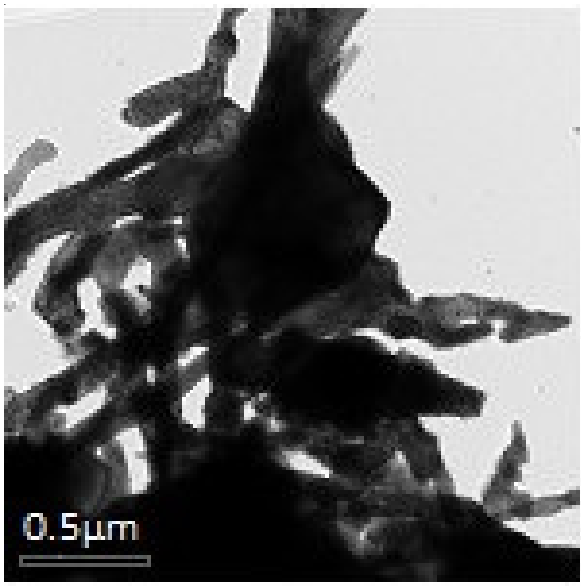

Fig. 3. TEM image of MoS_2-D

Fig. 4 shows the electron diffraction image of MoO_2 in MoS_2-D. There were many tiny fibres with regular diffraction rings on the surface of the MoO_2 crystal, indicating that the fibrous material was of tiny nano-crystalline form. It was confirmed that these small crystals belonged to the family of orthorhombic hexahedral molybdenum sulphide crystals through the *d*-value analysis of the diffraction ring.

Fig. 5 shows the TEM picture of MoS_2-A3 from where it can be seen that MoS_2-A3 was composed of countless, tiny, fibrous crystals dispersed evenly in an amorphous matrix. The average fibre length was 30 nm and width less than 3 nm. Each bundle of fibres was composed of about 2 to 5 fibres. The TEM image is a transmission image of the crystal in a plane, so these fibres were formed by small MoS_2 crystals which are built-up in layers in a flat panel stacking arrangement. The layered stacking structure was extremely important for catalytic hydrogenation and thus deep desulphurization.

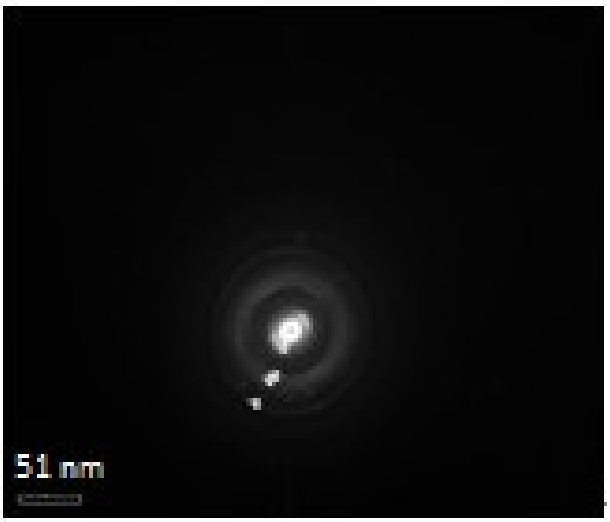

Fig. 4. Electron diffraction image of MoO_2 in MoS_2-D

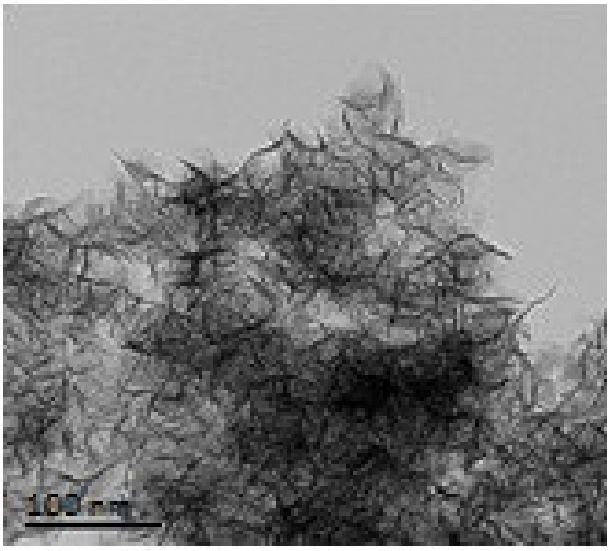

Fig. 5. Transmission electron micrograph of MoS_2-A3

Conclusion

The high-temperature hydrogen sulphide deoxidization and hydrothermal reduction were two types of more suitable methods for the synthesis of molybdenum sulphide powder. Infrared spectroscopy, Raman spectroscopy and TEM analysis results showed that the powder obtained from high-temperature hydrogen sulphide deoxidization was a mixture with, mainly, highly crystalline MoO_2 and less crystalline nano-MoS_2. MoS_2 fibres spread and grew to the centre of the MoO_2 crystal surface along the surface normal direction: the particle size was larger and more stacking manifest. Fibrous nano-molybdenum sulphide crystallization with high purity, high dispersivity and a uniform distribution, could be produced by the hydrothermal reduction method. The average fibre length was *ca.* 30 nm, with a width of less than 3 nm as evidenced by the processing of TEM images of the crystallized molybdenum sulphide. The molybdenum sulphide, MoS_2-A,as produced by hydrothermal reduction method, had the highest specific surface area, at up to 412.3 $m^2 g^{-1}$.

ACKNOWLEDGEMENTS

The authors acknowledged the support of Shaanxi Provincial Natural Science Funds (No.2012JM2011), the Scientific Research Programme Funded by Shaanxi Provincial Education Department (Program No.11JK0606,11JK0605) and the Key Subject Construction Programme for Chemical Engineering and Technology of Shaanxi Province Advanced Education.

REFERENCES

1. B.H. Liu, G.X. Yao and J. Liao, *J. Petrochem. Ind. Trends*, **12**, 27 (2001) in Chinese.
2. S.T. Oyama, P. Clark, X. Wang, T. Shido, Y. Iwasawa, S. Hayashi, J.M. Ramallo-López and F.G. Requejo, *J. Phys. Chem. B*, **106**, 1913 (2002).
3. M.K. Neylon, S.K. Bej, C.A. Bennett and and L.T. Thompson, *Appl. Catal*. A, **232**, 13 (2002).
4. M. Saito and R.B. Anderson, *J. Catal*., **63**, 438 (1980).
5. S. Ramanthan, C.C. Yu and S.T. Oyama, *J. Catal*., **173**, 10 (1998).
6. M.L. Xiang and D.B. Li, *J. Fuel Chem. Technol.*, **35**, 324 (2007).
7. G.Z. Jing, J.H. Zhu, X.J. Fan, G.D. Sun and J.B. Gao, *Chin. J. Catal.*, **27**, 899 (2006).
8. G.A. Camacho-Bragado, J.L. Elechiguerra, A. Olivas, S. Fuentes, D. Galvan and M.J. Yacaman, *J. Catal*., **234**, 182 (2005).
9. A.A. Tsyganenko, F. Can, A. Travert and F. Maugé, *Appl. Catal. A*, **268**, 189 (2004).